C. R. Chimie 14 (2011) 611–618

Contents lists available at ScienceDirect

Comptes Rendus Chimie

www.sciencedirect.com

Full paper/Mémoire

Synthesis, hydration and sintering of calcium aluminate nanopowder for advanced applications

Mahmoud F. Zawrah [a,*], Adel B. Shehata [b], Esam A. Kishar [c], Randa N. Yamani [b]

[a] National Research Center, Ceramic Department, 12622 Dokki, Cairo, Egypt
[b] National Institute of Standards, Reference Materials Department, 12211 El-haram, Giza, Egypt
[c] Faculty of Girls, Ain Shams University, Cairo, Egypt

ARTICLE INFO

Article history:
Received 18 June 2010
Accepted after revision 2 November 2010
Available online 6 January 2011

Keywords:
Calcium aluminate
Nanopowder
Synthesis
Hydration
Sintering

ABSTRACT

Seven batches of calcium aluminate powder containing different ratios of alumina and calcium oxide were chemically prepared by thermal decomposition method. The produced powder was investigated in terms of phase composition and morphology by XRD pattern and scanning electron microscope (SEM). The hydration and sintering of the prepared powder were also studied. Phase composition, microstructure and mechanical properties of the hydrated and sintered bodies were tested. The results revealed that the batches containing high CaO/Al_2O_3 ratios i.e., batches 1, 2 and 3 composed mainly of $CaO.Al_2O_3$ (CA) and $12CaO.7Al_2O_3$ ($C_{12}A_7$) phases while batches containing low CaO/Al_2O_3 ratios i.e., batches 4, 5, 6 and 7 composed of CA and CA_2 ($CaO.2Al_2O_3$) phases. The amount of these phases affected the properties of hydrated as well as the sintered bodies. The hydration of batches No. 1, 2 and 3 achieved higher strength than batches containing low CaO/Al_2O_3 ratios due to the presence of CA and $C_{12}A_7$ as a major component, since they react rapidly with water. The presence of $C_{12}A_7$ phase in the batches containing higher CaO/Al_2O_3 ratios decreased the apparent porosity and consequently increased the mechanical properties of the sintered bodies. The obtained materials can be applied for different advanced applications. The bioactivity of the obtained materials will be studied and published as a second part of this article.

1. Introduction

The term calcium aluminate cements (CAC) covers range of inorganic binders characterized by the presence of monocalcium aluminate CA ($CaO.Al_2O_3$) as their main constituent. Calcium aluminate cement is also called aluminous cement or high alumina cement. The chemical composition of calcium aluminate cement may vary over wide range of Al_2O_3 contents ranging between about 40% and 80%. Unlike Portland cement, it does not contain tricalcium silicate, but may contain limited amounts of dicalcium silicate. Compared with Portland cement, the annual production of calcium aluminate cements is very small. They are also more expensive. Calcium aluminate cements have several unique properties where the performance of Portland cement is insufficient. These properties include: rapid strength development even at low temperature, high temperature resistance refractory performance, and resistance to wide range of chemically aggressive conditions [1,2]. In recent years new applications for calcium aluminates have emerged in optical, bio and structural ceramics. Some amorphous calcium aluminate compositions are photosensitive and hence are potential candidates for optical information storage devices [3–6]. They also have very desirable infrared transmission properties for optical fiber applications [7,8]. Conventionally, calcium aluminate cement is produced by fusing limestone as a source of calcium oxide (CaO) and

* Corresponding author.
E-mail address: mzawrah@hotmail.com (M.F. Zawrah).

1631-0748/$ – see front matter © 2010 Published by Elsevier Masson SAS on behalf of Académie des sciences.
doi:10.1016/j.crci.2010.11.004

bauxite as a source of aluminium oxide (Al_2O_3) at high temperatures up to 1400 °C. The oxide composition of the blend may vary over a wide range depending on the type of calcium aluminate cement to be produced. The produced material is then ground to fine powder. CA is the main constituent of all types of calcium aluminate cement in addition to undesirable amounts of $CaAl_4O_7$, $Ca_{12}Al_{14}O_{33}$ in addition to the starting reactants. Wet chemical synthesis methods can be applied for the preparation of ceramic powders with special characteristics, such as high sinterability, high surface area, well-defined and controlled chemical compositions and homogeneous distribution of the elements. Alternative low temperature techniques such as sol–gel, polymeric precursor processes and combustion synthesis have been applied for the synthesis of calcium aluminate compounds, instead of solid-state synthesis [9–13]. The present work aims at the preparation and investigation of calcium aluminate nanopowder for advanced applications such as biomedical applications. Studying the hydration, phase composition and sintering of such kind of nanopowder was also the goal of this work.

2. Experimental

Hydrated aluminium nitrate $Al(NO_3)_3.9H_2O$ and hydrated calcium nitrate $Ca(NO_3)_2.4H_2O$ were used as starting materials for the preparation of monocalcium aluminate with different CaO/Al_2O_3 ratios. The batches were designed according to Table 1.

Aluminium nitrate and calcium nitrate masses were weighed and mixed with about 50 ml of water. The solution was heated on a sand bath up to 300 °C. After evaporation of water during continuous heating, brown fumes of nitrogen oxides were detected. The samples were left until all fumes disappeared and the mixture solidified again. A tough white solid was formed at the end of the heating process. The produced solids were calcined at 500 °C and 950 °C for 1 hour to study the effect of calcination temperature on the phase formation. The phase composition of the fired powders were determinate by XRD using Philips model Bruker D_8 Advance, Germany, with Cu Kα target and secondary monochromator, V = 40 kv, A = 40 mA. Ni filter. A SEM, Philips XL.30, Netherlands, was used to study the morphology and particle size of the powder calcined at 500 °C and 950 °C. Also Infrared analysis (IR) was used to identify the products.

Table 1
Molar ratios of CaO/Al_2O_3 for cement batches.

Batch No.	CaO/Al_2O_3 molar ratios
B1	1.05:1
B2	1.10:1
B3	1:1
B4	1:1.05
B5	1:1.10
B6	1:1.15
B7	1:1.20

The calcined powders prepared at 950 °C have been mixed with an adequate amount of water to form cement paste then casted in a cubic steel mould with dimensions of 1 × 1 × 1 cm using a vibrating table at frequency 50 Hz and 4 min vibrating time and kept under 100% relative humid conditions for 30 days. They were then removed from water, dried and tested for cold crushing strength [14].

The produced calcium aluminate powders were pressed at 50 MPa and sintered in an electrical furnace between 1350 °C and 1550 °C. Densification parameters in terms of bulk density and apparent porosity were determined by Archimeds methods. XRD and SEM were also used for

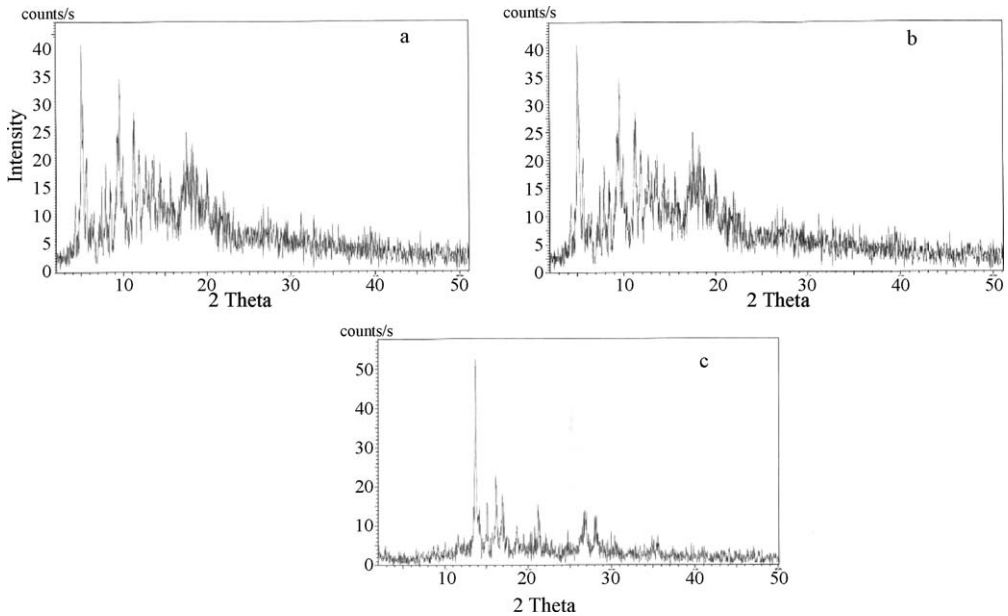

Fig. 1. XRD patterns of as-prepared calcium aluminate powder (a), calcined at 500 °C (b) and 950 °C (c), respectively.

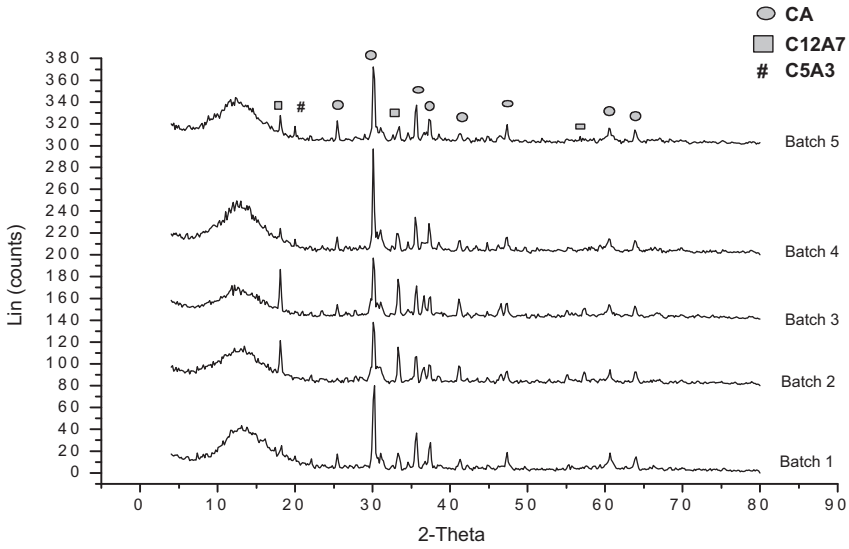

Fig. 2. XRD pattern of the calcium aluminate batches calcined at 950 °C.

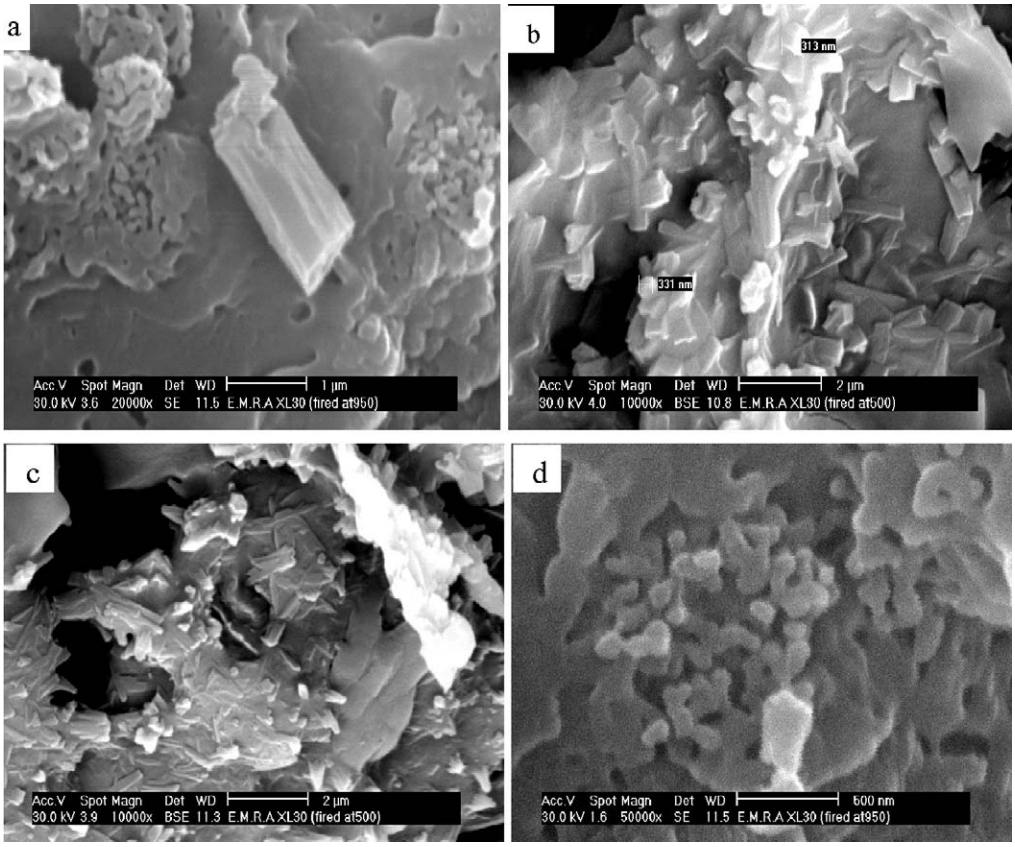

Fig. 3. SEM photomicrographs of CA, batch No. 1 calcined at 500 °C (a, b) and 950 °C (c, d).

analysis of phase composition and microstructure of sintered and hydrated samples. The mechanical properties i.e., cold crushing strength was examined by a hydraulic testing machine.

3. Results and discussion

3.1. Characterization of the chemically prepared batches

3.1.1. Phase composition

The effect of calcination temperature on the phase formation of the as-prepared calcium aluminate cement (batch No. 3, 1:1 CaO/Al_2O_3 molar ratio) and those calcined at 500 °C as well as 950 °C are shown in Fig. 1. It is indicated that the as-prepared sample is an amorphous and sign initial formation of crystalline phases of calcium aluminate. At 500 °C, the amorphousity is decreased and some peaks characterizing monocalcium aluminate are detected. At 950 °C, peaks of crystalline monocalcium aluminate appeared with small amounts of dodeca-calcium hepta aluminate ($C_{12}A_7$). XRD spectra of all prepared batches calcined at 950 °C are shown in Fig. 2. It appears that the monocalcium aluminate phase (CaO. Al_2O_3) is the major constituent of the prepared calcium aluminate binary system, but its quantity varies between batches according to their aluminium oxide to calcium oxide molar ratios [3]. Also it is indicated that a dodeca-calcium hepta aluminate phase ($C_{12}A_7$) is formed in all batches. For the batches 4, 5, 6 and 7, a new phase is formed which is C_5A_3 (5CaO. $3Al_2O_3$). This phase is stable only in the absence of humidity and oxygen. Under normal moisture, it composes rapidly to CA and $C_{12}A_7$ [9,15–17].

3.1.2. Microstructure of the prepared powders

Fig. 3 shows SEM micrographs of calcium aluminate cement (batch No. 1) calcined at 500 °C and 950 °C. Small crystals are formed in the nanorange with different shapes and particle size distribution which indicates the formation of heterogeneous materials. This is due to the formation of different phases as shown in XRD.

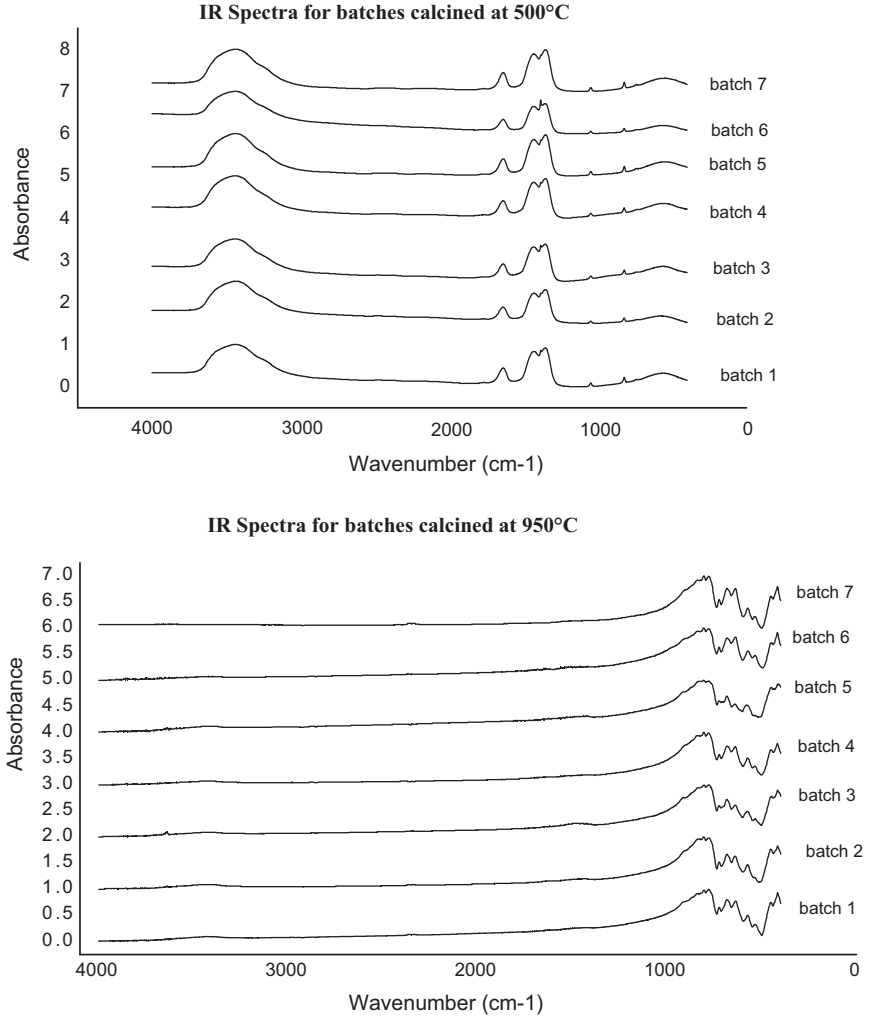

Fig. 4. IR Spectra of calcium aluminate powders calcined at 500 °C and 950 °C.

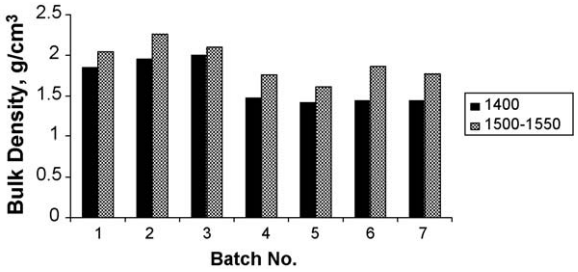

Fig. 5. Bulk density of the samples sintered at two different temperatures.

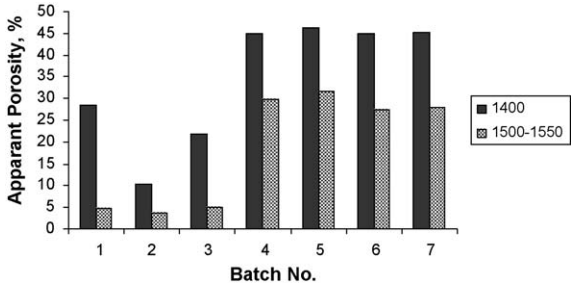

Fig. 6. Apparent porosity of the samples sintered at two different temperatures.

3.1.3. FTIR spectroscopy

The FTIR spectra of the samples as a function of calcinations temperature are given in Fig. 4. It is indicated that, in the samples fired at 500 °C, broad peaks are formed at 3400 cm^{-1} and 1700–1600 cm^{-1} due to O–H stretching and bending vibration. This is due to the presence of water molecules absorbed on the surface of the highly reactive calcium aluminate. Also, other peaks are formed at 1400–1300 and 860–800 cm^{-1} due to the presence of NO_3^- from the starting materials. This means that the sample needs longer calcination time or higher temperatures to remove all nitrates. In the samples fired at 950 °C, all peaks have disappeared due to the complete reaction between aluminium and calcium nitrates and new peaks are formed in the fingerprint region (less than 1000 cm^{-1}) due to the vibrations of tetrahedron AlO_4 and octahedron AlO_6 [18,19].

3.2. Characterization of sintered and hydrated pellets

3.2.1. Bulk density and apparent porosity of the sintered pellets

Results of the bulk density and apparent porosity of the batches sintered at two different temperatures are represented graphically in Figs. 5 and 6 respectively. It appears that, the bulk density increases with increasing the firing temperature. Also, it is found that the first three batches exhibited higher bulk density as compared with the other batches. This is due to the variation of CaO/A_2O_3 molar ratio, which consequently affects the type and amount of the formed phases. In the first three batches, the formed phases are CA and $C_{12}A_7$ (melting point, 1600 and 1360–1390 °C, respectively) while in the other four batches; the formed phases are CA and CA_2 (melting point, 1600 and 1750–1765 °C, respectively).

In constrast, the apparent porosity decreases with increasing the firing temperature and the first three batches gave lower apparent porosity as compared with the other four batches. So these batches need further firing at higher temperature in order to get a lower value of the apparent porosity.

3.2.2. Phase composition

Fig. 7 exhibits XRD pattern of the sintered samples. From the figure, it appears that CA is the major constituent in all batches with different quantities according to aluminium oxide to calcium oxide ratios. Also, small

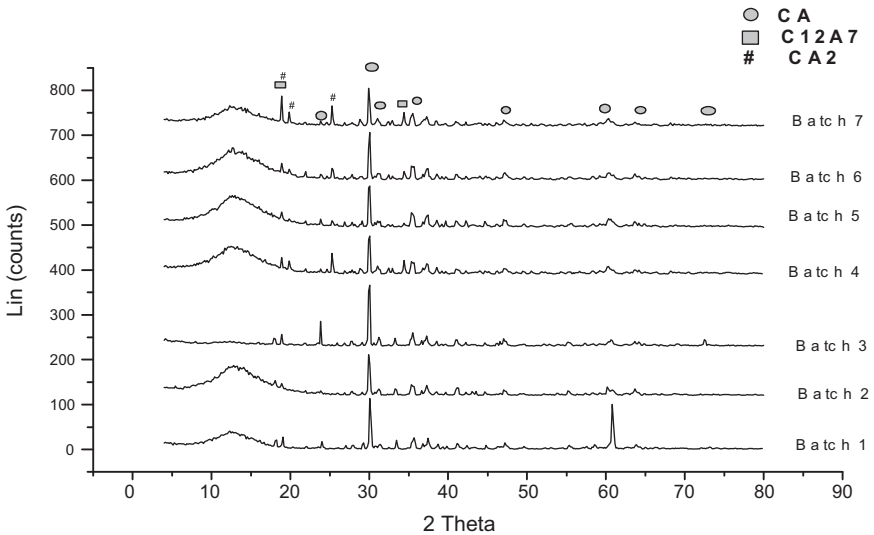

Fig. 7. XRD pattern of the sintered batches at 1550 °C.

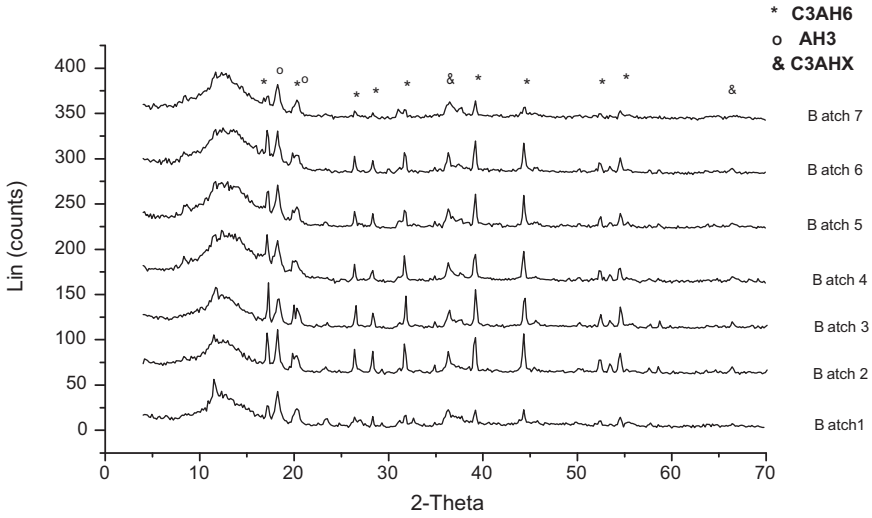

Fig. 8. XRD pattern of the hydrated batches.

amounts of CA_2 are detected in the batches 4, 5, 6 and 7, whereas small amounts of $C_{12}A_7$ are formed in the batches 1, 2 and 3.

Fig. 8 shows XRD pattern of the hydrated batches. $CaO.Al_2O_3.10H_2O$ (CAH_{10}) and $2CaO.Al_2O_3.8H_2O$ (C_2AH_8) phases are known to be the main hydration product of CA, CA_2 and $C_{12}A_7$ and they play the bonding role in such materials. The higher C/A ratio of $C_{12}A_7$ favors the formation of C_2AH_8 with very little amounts of CAH_{10}. By increasing the hydration time, all phases are converted into C_3AH_6. Alumina gel $Al(OH)_3$ (AH_3) was generally observed as structureless grains [20].

3.2.3. Mechanical properties of hydrated and sintered calcium aluminate

Fig. 9 exhibits cold crushing strength of the sintered samples. It is indicated that, for batches 4, 5, 6 and 7, the strength is lower than those of the batches 1, 2 and 3. This is due to the higher content of CaO in these batches and consequently formation of $C_{12}A_7$ phase, which has low melting point. This phase close the pores between the grains, so increase the strength of these batches, while batches 4, 5, 6 and 7, contain higher amounts of CA_2 phase. High short-term strength is relatively exhibited by the formation of $C_{12}A_7$, whereas the long-term strength increases with increasing CA content.

Fig. 10 shows cold crushing strength of the hydrated calcium aluminate. Hydrated batches No. 1, 2 and 3 achieved higher strength than batches 4, 5 and 6. This is due to the presence of CA and $C_{12}A_7$ as a major component, since they react rapidly with water. It is well known that CA and $C_{12}A_7$ react significantly at early ages of hydration. So, batches No. 1, 2 and 3 gained higher strength at early stages of hydration as compared with batches 4, 5 and 6, which contain CA and CA_2 as major phases. CA_2 is known to react slowly with water in the early stages of hydration. The presence of CA_2 along with CA results in overall faster hydration rate as the heat of hydration resulting from the hydration of CA activates CA_2 and makes it react relatively faster with water than it would do alone. So due to the poor hydration of CA_2 at the early hydration stage, batches 4, 5 and 6 gave lower strength [21,22].

3.2.4. Microstructure of sintered and hydrated calcium aluminate

The morphology and microstructure of the sintered samples (batches 2, 3 and 7) are shown in Fig. 11. The

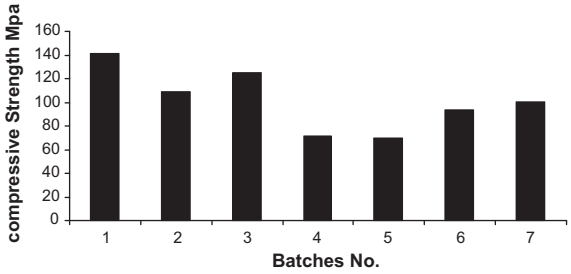

Fig. 9. Cold crushing strength of the sintered calcium aluminate at 1550 °C.

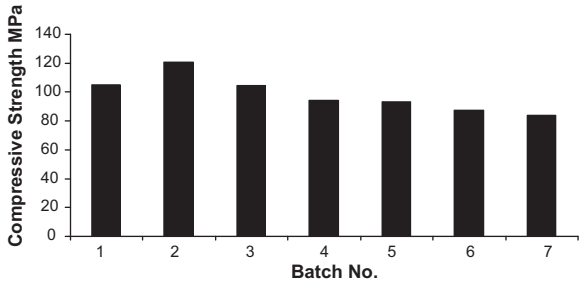

Fig. 10. Cold crushing strength of the hydrated calcium aluminate.

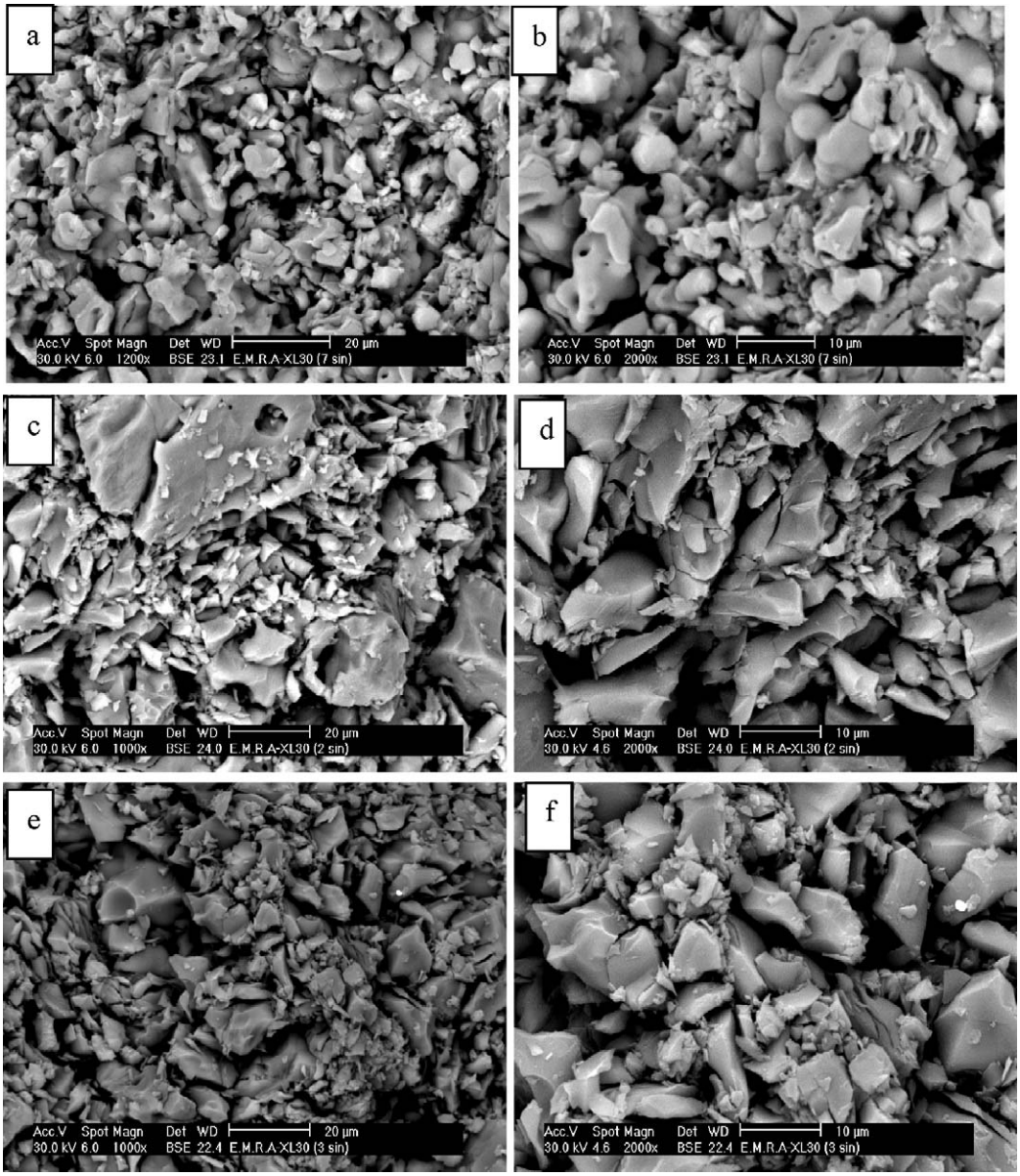

Fig. 11. SEM photomicrographs of the sintered samples at 1550 °C, (a, b) batch No. 2, (c, d) batch No. 3 and (e, f) batch No. 7.

photomicrographs show wide range of particle size in all batches with non-regular shape. Euhedral and edged CA grains are detected in all batches. Their amounts decrease as we going from batch No. 3 into batch No. 7. Also, the batch No. 2 showed lower porosity as compared with batches 3 and 7. This means that the firing temperature (1550 °C) is not enough to get the minimum porosity and the maximum bulk density. As mentioned before and indicated from the photomicrographs, the porosity of all samples is still high. The batch No. 7 exhibited relatively homogeneous grain-sized microstructure as compared with the batches No. 3. This homogeneous grain-sized microstructure leads to enhancement of the compressive strength as compared with the batches No. 4 and 5.

Fig. 12 shows SEM photomicrographs of the hydrated batches at different magnifications. A denser structure with homogeneous grain size is formed in batch No. 3 which contains CA and $C_{12}A_7$ as compared with batch No. 7 which contains CA and CA_2 phases. This is due to the fast reaction of CA and $C_{12}A_7$ with water at early ages of hydration, in addition to its very exothermic hydration characteristic. So the formation of stable hydrates occurs sooner. Although CA_2 is known to react slowly with water in the early stages of hydration the presence of CA activates CA_2 and makes it react relatively faster with water than it would do alone [3].

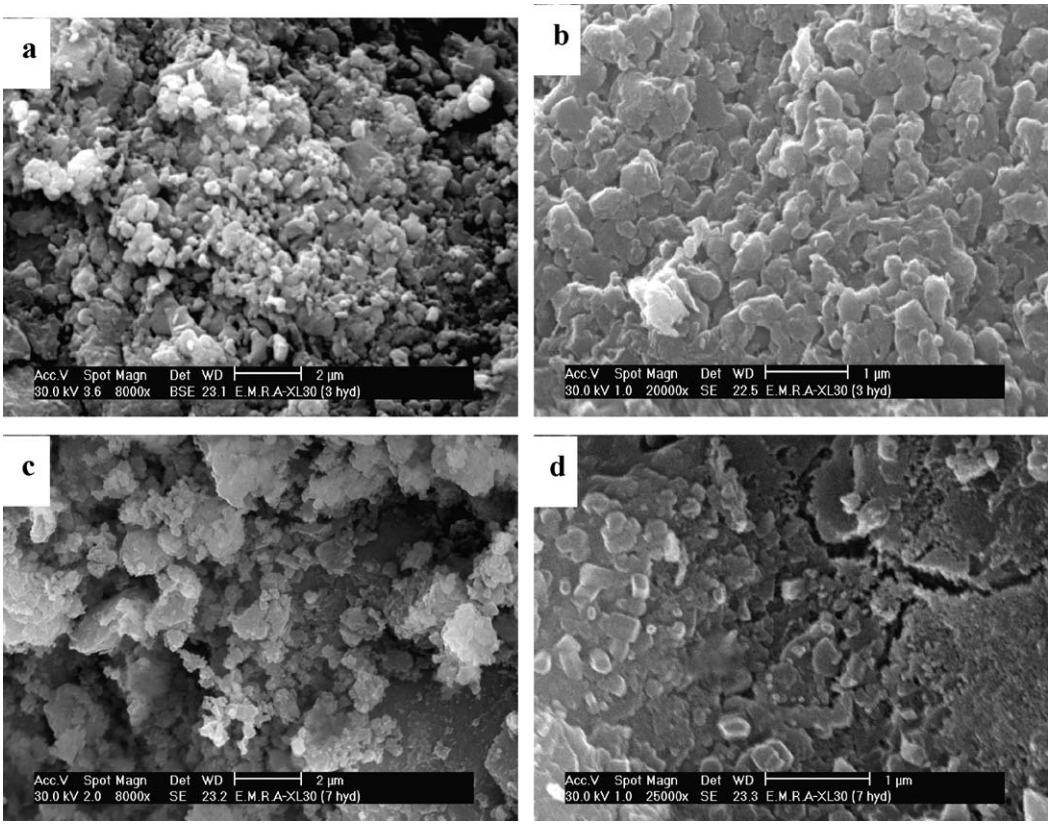

Fig. 12. SEM photomicrographs of hydrated batches, (a, b) batch No. 3 and (c, d) batch No. 7.

4. Conclusions

It is concluded that the batches 1, 2 and 3 which have higher CaO/Al_2O_3 molar ratios, composed mainly of CA and $C_{12}A_7$ phases while batches 4, 5, 6 and 7 which have higher CaO/Al_2O_3 molar ratios, composed of CA and CA_2 phases. The amount of these phases affects the properties of hydrated as well as the sintered calcium aluminate. Also the first three batches exhibited higher bulk density and lower apparent porosity as compared with the other batches. This is due to the variation of CaO/A_2O_3 molar ratios and consequently formation of low melting phase ($C_{12}A_7$), which close the pores in the first three batches more than the other batches. After sintering process, the obtained nanopowder is converted to microsized grains due to the grain growth developed by heat treatment. Extra study is needed to control the grain size to nanosize after sintering process.

References

[1] J.J. Bensted, P. Bares, Structure and Performance of Cements, second ed., Spon Press, 2002.
[2] Lea, Lea's Chemistry of Cement and Concrete, edited by Peter C. Hewlett, fourth ed., Arnold, 1998.
[3] M.F. Zawrah, N.M. Khalil, Ceram. Int. (2006) 1.
[4] M.A. Gulgun, O.O. Popoola, W.M. Kriven, J. Am. Ceram. Soc. 77 (2) (1994) 531.
[5] F.T. Wallenberger, N.E. Weston, S.D. Brown, in: Proceedings of the Society of Photo-Optical Instrumentation Engineers, vol. 1484, Growth and Characterization of Materials for Infrared Detectors, SPIE—The International Society for Optical Engineering, Bellingham, WA, 1991, pp. 116.
[6] J.D. Birchall, A.J. Howard, K. Kendall, Nat. (Lond.) 289 (1981) 388.
[7] K. Kendall, J.D. Birchall, A.J. Howard, Philos. Trans. R. Soc. A310 (1983) 139.
[8] A.A. Goktas, M.C. Weinberg, J. Am. Ceram. Soc. 74 (5) (1991) 1066.
[9] A. Gaki, R. Chrysafi, G. Kakali, J. Eur. Ceram. Soc. (2007) 1781.
[10] K. Fujji, W. Kondo, H. Ueno, J. Am. Ceram. Soc 69 (4) (1986) 361.
[11] R.N. Edmonds, A.J. Majumdar, Cem. Concr. Res. 18 (1988) 311.
[12] M. Uberoi, S.H. Risbud, J. Am. Ceram. Soc. 73 (56) (1990) 1768.
[13] D.M. Roy, R.R. Neurgaonkar, T.P. O'Holleran, R. Roy, Am. Ceram. Soc. Bull. 56 (11) (1977) 1023.
[14] R.E. Fisher, Am. Ceram. Soc. (1992).
[15] V.K. Singh, M.M. Ali, U.K. Mandal, J. Am. Ceram. Soc. 73 (4) (1990) 872.
[16] V.K. Singh, M.M. Ali, J. Br. Ceram. Soc. 79 (1980) 112.
[17] V.K. Singh and U.K. Mandal, Trans. J. Br. Ceram. Soc. 81 (4) (1982) 112.
[18] Ivan Odler, Special Inorganic Cements, Spon Press, UK, 2000pp. 175.
[19] B. Stuart, Infrared Spectroscopy: Fundamentals and Applications, John Wiley & Sons Ltd, 2004.
[20] J.H. Park, D.J. Min, H.S. Song, ISIJ Int. 42 (2002) 38.
[21] M.F. Zawrah, N.M. Khalil, Br. Ceram. Trans. 101 (5) (2002).
[22] M. Nilforoushan, T. Reza, Nasrien, Iran. J. Chem. Chem. Eng. (2007) 71.